

FERMI/LAT DISCOVERY OF GAMMA-RAY EMISSION FROM A RELATIVISTIC JET IN THE
NARROW-LINE QUASAR PMN J0948+0022

A. A. Abdo^{1,2}, M. Ackermann³, M. Ajello³, M. Axelsson^{4,5}, L. Baldini⁶, J. Ballet⁷, G. Barbiellini^{8,9},
D. Bastieri^{10,11}, M. Battelino^{4,12}, B. M. Baughman¹³, K. Bechtol³, R. Bellazzini⁶, E. D. Bloom³,
E. Bonamente^{14,15}, A. W. Borgland³, J. Bregeon⁶, A. Brez⁶, M. Brigida^{16,17}, P. Bruel¹⁸, G. A. Calciandro^{16,17},
R. A. Cameron³, P. A. Caraveo¹⁹, J. M. Casandjian⁷, E. Cavazzuti²⁰, C. Cecchi^{14,15}, A. Chekhtman^{2,21},
C. C. Cheung²², J. Chiang³, S. Ciprini^{14,15}, R. Claus³, J. Cohen-Tanugi²³, W. Collmar²⁴, J. Conrad^{4,12,25,26},
L. Costamante³, C. D. Dermer², A. de Angelis²⁷, F. de Palma^{16,17}, S. W. Digel³, E. do Couto e Silva³,
P. S. Drell³, R. Dubois³, D. Dumora^{28,29}, C. Farnier²³, C. Favuzzi^{16,17}, W. B. Focke³, L. Foschini^{30,*}, M. Frailis²⁷,
L. Fuhrmann³¹, Y. Fukazawa³², S. Funk³, P. Fusco^{16,17}, F. Gargano¹⁷, N. Gehrels^{22,33}, S. Germani^{14,15},
B. Giebels¹⁸, N. Giaretta^{16,17}, F. Giordano^{16,17}, M. Giroletti³⁴, T. Glanzman³, I. A. Grenier⁷,
M. H. Grondin^{28,29}, J. E. Grove², L. Guillemot^{28,29}, S. Guiriec³⁵, Y. Hanabata³², A. K. Harding²²,
R. C. Hartman²², M. Hayashida³, E. Hays²², R. E. Hughes¹³, G. Johannesson³, A. S. Johnson³, R. P. Johnson³⁶,
W. N. Johnson², T. Kamae³, H. Katagiri³², J. Kataoka³⁷, M. Kerr³⁸, J. Knodlseder³⁹, F. Kuehn¹³, M. Kuss⁶,
J. Lande³, L. Latronico⁶, M. Lemoine-Goumard^{28,29}, F. Longo^{8,9}, F. Loparco^{16,17}, B. Lott^{28,29}, M. N. Lovellette²,
P. Lubrano^{14,15}, G. M. Madejski³, A. M. M. Akeev^{2,21}, W. M. Max-Moerbeck⁴⁰, M. N. M. Azzotta¹⁷, W. M. C. Conville^{22,33},
J. E. McEnery²², C. Meurer^{4,25}, P. F. Michelson³, W. M. Mithumsiri³, T. Mizuno³², C. Monte^{16,17}, M. E. Monzani³,
A. Morselli⁴¹, I. V. Moskaleenko³, S. Murgia³, P. L. Nolan³, J. P. Norris⁴², E. Nuss²³, T. Ohsugi³², N. Omodei⁶,
E. Orlando²⁴, J. F. Ormes⁴², D. Paneque³, J. H. Panetta³, D. Parent^{28,29}, V. Pavlidou⁴⁰, T. J. Pearson⁴⁰,
M. Pepe^{14,15}, M. Pesce-Rollins⁶, F. Piron²³, T. A. Porter³⁶, S. Raino^{16,17}, R. Rando^{10,11}, M. Razzano⁶,
A. Readhead⁴⁰, A. Reimer³, O. Reimer³, T. Reposeur^{28,29}, J. L. Richards⁴⁰, S. Ritz²², A. Y. Rodriguez⁴³,
R. W. Romani³, F. Ryde^{4,12}, H. F. W. Sadrozinski³⁶, R. Sambruna²², D. Sanchez¹⁸, A. Sander¹³,
P. M. Saz Parkinson³⁶, J. D. Scargle⁴⁴, T. L. Schalk³⁶, C. Sgrò⁶, D. A. Smith^{28,29}, G. Spandre⁶, P. Spinelli^{16,17},
J.-L. Starck⁷, M. Stevenson⁴⁰, M. S. Strickman², D. J. Suson⁴⁵, G. Tagliaferri³⁰, H. Takahashi³², T. Tanaka³,
J. G. Thayer³, D. J. Thompson²², L. Tibaldo^{10,11}, O. Tibolla⁴⁶, D. F. Torres^{43,47}, G. Tosti^{14,15}, A. Tramacere^{3,48},
Y. Uchiyama³, T. L. Usher³, N. Vilchez³⁹, V. Vitale^{41,49}, A. P. Waite³, B. L. Winer¹³, K. S. Wood²,
T. Y. Linen^{4,12,50}, J. A. Zensus³¹, M. Ziegler³⁶ (The Fermi/LAT Collaboration)
and
G. Ghisellini³⁰, L. Maraschi³⁰, F. Tavecchio³⁰, E. Angelakis³¹

Draft version August 12, 2024

ABSTRACT

We report the discovery by the Large Area Telescope (LAT) onboard the Fermi Gamma-ray Space Telescope of high-energy γ ray emission from the peculiar quasar PMN J0948+0022 ($z = 0.5846$). The optical spectrum of this object exhibits rather narrow H β (FWHM(H β) = 1500 km s⁻¹), weak forbidden lines and is therefore classified as a narrow-line type I quasar. This class of objects is thought to have relatively small black hole mass and to accrete at high Eddington ratio. The radio loudness and variability of the compact radio core indicates the presence of a relativistic jet. Quasi-simultaneous radio-optical-X-ray and γ -ray observations are presented. Both radio and γ -ray emission (observed over 5 months) are strongly variable. The simultaneous optical and X-ray data from Swift show a blue continuum attributed to the accretion disk and a hard X-ray spectrum attributed to the jet. The resulting broad band spectral energy distribution (SED) and, in particular, the γ -ray spectrum measured by Fermi are similar to those of more powerful FSRQ. A comparison of the radio and γ -ray characteristics of PMN J0948+0022 with the other blazars detected by LAT shows that this source has a relatively low radio and γ -ray power, with respect to other FSRQ. The physical parameters obtained from modelling the SED also fall at the low power end of the FSRQ parameter region discussed in Celotti & Ghisellini (2008). We suggest that the similarity of the SED of PMN J0948+0022 to that of more massive and more powerful quasars can be understood in a scenario in which the SED properties depend on the Eddington ratio rather than on the absolute power.

Subject headings: quasars: individual (PMN J0948+0022) { galaxies: active { gamma rays: observations

* Corresponding author: luigi.foschini@brera.inaf.it.

¹ National Research Council Research Associate

² Space Science Division, Naval Research Laboratory, Washington, DC 20375

³ W. W. Hansen Experimental Physics Laboratory, Kavli Institute for Particle Astrophysics and Cosmology, Department of Physics and SLAC National Accelerator Laboratory, Stanford University, Stanford, CA 94305

⁴ The Oskar Klein Centre for Cosmoparticle Physics, Alnabova,

SE-106 91 Stockholm, Sweden

⁵ Department of Astronomy, Stockholm University, SE-106 91 Stockholm, Sweden

⁶ Istituto Nazionale di Fisica Nucleare, Sezione di Pisa, I-56127 Pisa, Italy

⁷ Laboratoire AIM, CEA-IRFU/CNRS/Université Paris Diderot, Service d'Astrophysique, CEA Saclay, 91191 Gif sur Yvette, France

⁸ Istituto Nazionale di Fisica Nucleare, Sezione di Trieste,

1. INTRODUCTION

It is now widely recognised that strong radio sources associated with active galactic nuclei (AGN) must be powered by collimated relativistic energy flows (Rees 1966). The bulk Lorentz factors (Γ) of these flows may be different in different systems and at different distances from the active nucleus. If a blob of plasma moving at relativistic speed is observed at small angles to the

jet axis ($\theta \ll 1/\Gamma$) the observed radiation is amplified and the timescales shortened due to relativistic effects. Such systems are generically called blazars (Blanford & Rees 1978). Blazars have been often classified in subcategories: Flat-Spectrum Radio Quasars (FSRQ), characterized by strong and broad optical emission lines, and BL Lac objects, when no emission lines are apparent above the optical/UV continuum (e.g. Urry & Padovani 1995).

Remarkably, the Compton Gamma-Ray Observatory (CGRO) together with the first generation of Cherenkov Telescopes discovered that the SED of a number of the brightest blazars extend to the γ -ray range, showing two broad components: the first one, covering radio to soft X-rays, is thought to be due to the synchrotron emission from relativistic electrons, while the second one, covering the hard X-/ γ -ray band, is generally attributed to inverse-Compton (IC) emission. The seed photons for the IC process can originate from the synchrotron radiation itself (synchrotron self-Compton, SSC; e.g. Ghisellini et al. 1985) or from an external source, like the accretion disk, the broad-line region or a dusty torus (external Compton, EC; e.g. Derm er et al. 1992, Sikora et al. 1994, Blazejowski et al. 2000).

Compiling and averaging the SED of the brightest blazars, Fossati et al. (1998) found an interesting trend { the blazar sequence { whereby for sources with low bolometric luminosity both components peak at high frequencies (UV/soft X-rays for synchrotron and TeV for IC { High-frequency peaked BL Lacs, HBL), while, for increasing luminosities, both peaks shift to lower frequencies (Low-frequency peaked BL Lacs, LBL and FSRQ).

Ghisellini et al. (1998) proposed to explain the sequence in terms of correlation between the random Lorentz factor of electrons emitting at the peaks of the SED (Γ_{peak}) and the global energy density (U) in the comoving frame. HBL have low U and high Γ_{peak} , while FSRQ have high U and low Γ_{peak} . The sequence can also be interpreted in an evolutionary frame (Botcher & Derm er 2002, Cavaliere & D'Elia 2002).

It is important to stress that the selection of objects with which the sequence was constructed was admittedly biased by the available samples, within which only a limited number of objects had γ -ray data (Maraschi & Tavecchio 2001). In fact challenges have been raised to the validity of the sequence (for a review, see Padovani 2007 and references therein), which however could be overcome (Maraschi et al. 2008, Ghisellini & Tavecchio 2008). Today, the ongoing Fermi mission is expected to provide a deeper and unbiased survey of the whole γ -ray sky, compared to that available during the

I-34127 Trieste, Italy

⁹ Dipartimento di Fisica, Università di Trieste, I-34127 Trieste, Italy

¹⁰ Istituto Nazionale di Fisica Nucleare, Sezione di Padova, I-35131 Padova, Italy

¹¹ Dipartimento di Fisica "G. Galilei", Università di Padova, I-35131 Padova, Italy

¹² Department of Physics, Royal Institute of Technology (KTH), Albanova, SE-106 91 Stockholm, Sweden

¹³ Department of Physics, Center for Cosmology and Astrophysics, The Ohio State University, Columbus, OH 43210

¹⁴ Istituto Nazionale di Fisica Nucleare, Sezione di Perugia, I-06123 Perugia, Italy

¹⁵ Dipartimento di Fisica, Università degli Studi di Perugia, I-06123 Perugia, Italy

¹⁶ Dipartimento di Fisica "M. Merlin" dell'Università e del Politecnico di Bari, I-70126 Bari, Italy

¹⁷ Istituto Nazionale di Fisica Nucleare, Sezione di Bari, 70126 Bari, Italy

¹⁸ Laboratoire Leprince-Ringuet, Ecole polytechnique, CNRS/IN 2P 3, Palaiseau, France

¹⁹ INFN-Istituto di Astrofisica Spaziale e Fisica Cosmica, I-20133 Milano, Italy

²⁰ Agenzia Spaziale Italiana (ASI) Science Data Center, I-00044 Frascati (Roma), Italy

²¹ George Mason University, Fairfax, VA 22030

²² NASA Goddard Space Flight Center, Greenbelt, MD 20771

²³ Laboratoire de Physique Théorique et Astroparticules, Université Montpellier 2, CNRS/IN 2P 3, Montpellier, France

²⁴ Max-Planck Institut für extraterrestrische Physik, 85748 Garching, Germany

²⁵ Department of Physics, Stockholm University, Albanova, SE-106 91 Stockholm, Sweden

²⁶ Royal Swedish Academy of Sciences Research Fellow, funded by a grant from the K.A.W. Allenberg Foundation

²⁷ Dipartimento di Fisica, Università di Udine and Istituto Nazionale di Fisica Nucleare, Sezione di Trieste, Gruppo Collegato di Udine, I-33100 Udine, Italy

²⁸ CNRS/IN 2P 3, Centre d'Études Nucleaires Bordeaux-Mérignan, UMR 5797, Gargagnan, 33175, France

²⁹ Université de Bordeaux, Centre d'Études Nucleaires Bordeaux-Mérignan, UMR 5797, Gargagnan, 33175, France

³⁰ INFN Osservatorio Astronomico di Brera, I-23807 Merate, Italy

³¹ Max-Planck-Institut für Radioastronomie, Auf dem Hügel 69, 53121 Bonn, Germany

³² Department of Physical Sciences, Hiroshima University, Higashi-Hiroshima, Hiroshima 739-8526, Japan

³³ University of Maryland, College Park, MD 20742

³⁴ INFN Istituto di Radioastronomia, 40129 Bologna, Italy

³⁵ University of Alabama in Huntsville, Huntsville, AL 35899

³⁶ Santa Cruz Institute for Particle Physics, Department of Physics and Department of Astronomy and Astrophysics, University of California at Santa Cruz, Santa Cruz, CA 95064

³⁷ Waseda University, 1-104 Totsukamachi, Shinjuku-ku, Tokyo, 169-8050, Japan

³⁸ Department of Physics, University of Washington, Seattle, WA 98195-1560

³⁹ Centre d'Étude Spatiale des Rayonnements, CNRS/UPS, BP 44346, F-30128 Toulouse Cedex 4, France

⁴⁰ California Institute of Technology, Pasadena, CA 91125

⁴¹ Istituto Nazionale di Fisica Nucleare, Sezione di Roma "Tor Vergata", I-00133 Roma, Italy

⁴² Department of Physics and Astronomy, University of Denver, Denver, CO 80208

⁴³ Institut de Ciències de l'Espai (IEEC-CSIC), Campus UAB, 08193 Barcelona, Spain

⁴⁴ Space Science Division, NASA/Ames Research Center, Moffett Field, CA 94035-1000

⁴⁵ Department of Chemistry and Physics, Purdue University Calumet, Hammond, IN 46323-2094

⁴⁶ Max-Planck-Institut für Kernphysik, D-69029 Heidelberg, Germany

⁴⁷ Institutio Catalana de Recerca i Estudis Avançats (ICREA), Barcelona, Spain

⁴⁸ Consorzio Interuniversitario per la Fisica Spaziale (CIFS), I-10133 Torino, Italy

⁴⁹ Dipartimento di Fisica, Università di Roma "Tor Vergata", I-00133 Roma, Italy

⁵⁰ School of Pure and Applied Natural Sciences, University of Kalmar, SE-391 82 Kalmar, Sweden

CGRO/EGRET era, yielding possible surprises, as we will show in the present work.

Although the origin of relativistic jets is presently still not understood, there is increasing evidence that the properties of jets are related to the properties of the accretion flow which feeds the central black hole. In the case of stellar mass black holes the observed phenomenology points to an association of jet launching with accretion "modes" characterized by different spectral and timing properties (Fender & Belloni 2004). In the extragalactic domain the separation of radio sources into two broad classes (FR I and FR II), as well as the properties of their respective "beamed" representatives, BL Lacs and FSRQ, can be basically understood within a scenario based on the accretion mode: in the first class accretion onto the central black hole is sub-critical (in Eddington units) leading to radiatively inefficient accretion flows and relatively weak jets, while in the second one the accretion rate is near critical, giving rise to bright disks and powerful jets (Ghisellini & Celotti 2001, Maraschi 2001, Maraschi & Tavecchio 2003; see, however, also Blandford & Levinson 1995).

In this respect, the case of radio-loud narrow line Seyfert 1 (NLS1) active nuclei has received increasing attention. NLS1 are characterized by an optical spectrum with narrow permitted lines FWHM ($H\beta$) < 2000 km/s, the ratio between $[O III] \lambda 5007$ and $H\beta$ smaller than 3 and a bump due to FeII (see, e.g., Pogge 2000 for a review). They exhibit also prominent soft X-ray excesses. These properties point to very high (near Eddington) accretion rates and relatively low masses ($10^6 - 10^8 M_\odot$) (Boroson 2002; see, however, Decarli et al. 2008, Marconi et al. 2008). Only a small percentage of NLS1 are radio-loud (RL = $(S_{4.85GHz}/S_{440nm}) > 10$) or very radio-loud (RL > 100) (7% and 2.5% respectively). Their at radio spectra suggest that several of them could host relativistic jets: in fact VLB I variability indicates extremely high brightness temperatures and in some cases superluminal expansion has been observed (Komossa et al. 2006, Doi et al. 2006).

Recently, Yuan et al. (2008) studied a complete sample of radio-loud NLS1 selected from the Sloan Digital Sky Survey (SDSS) sample. They find that a large fraction of those for which X-ray data exist show broad band spectra similar to those of HBL, with peaks close to the UV band. The study of simultaneous optical/UV/X-ray data of a sample of radio-loud NLS1 revealed that these sources often display a hard X-ray component, especially in bright optical and ultraviolet states, thus supporting the possible contribution of a relativistic jet, in some cases similar to FSRQ (Foschini et al. 2009).

This class of sources thus is of extreme interest for extending the studies of the properties of relativistic jets to different mass and power scales. While it is clear that the most radio-loud NLS1 should host relativistic jets, the properties of such jets at high energy are essentially unknown. Observations of a few selected sources in the TeV energy range with the Whipple and HESS Cerenkov telescopes were performed, but yielded only upper limits (Falcone et al. 2004, Aharonian et al. 2008). A detection at high energy (GeV or TeV γ -rays) is essential to complete the knowledge about the SED, allowing to constrain the inverse-Compton parameters and discuss

analogies and differences with previously known blazars.

Here we present the first detection, by the Fermi/LAT, of γ rays from one of these radio-loud NLS1, the quasar PM N J0948+ 0022 ($z = 0.5846$). This makes it possible to build the first whole SED from radio to γ rays of a radio-loud NLS1, to constrain the inverse-Compton emission, and to evaluate the role of this new type of source in the framework of the blazar sequence and evolution. The paper is organized as follows: after a short identity card of the source in Sect. 2, the analysis of Fermi/LAT, Swift, Eelsberg and Owens Valley Radio Observatory data is presented in Sect. 3; Sect. 4 deals with the SED and the model selected to fit to the broadband spectrum, while the discussion and conclusions are given in Sect. 5. Throughout this work, we adopted a Λ CDM cosmology from the most recent WMAP results, which give the following values for the cosmological parameters: $h = 0.71$, $\Omega_m = 0.27$, $\Omega_b = 0.046$ and with the Hubble-Lemaître constant $H_0 = 100h \text{ km s}^{-1} \text{ Mpc}^{-1}$ (Komatsu et al. 2009).

2. THE SOURCE PM N J0948+ 0022

First identified in the M II-Green Bank radio survey at 5 GHz (Bennett et al. 1986), this quasar is part of the sample drawn from the SDSS and FIRST (Faint Images of the Radio Sky at Twenty-Centimeters) in a systematic search for radio loud NLS1 objects (Zhou et al. 2003, Komossa et al. 2006, Zhou et al. 2006, Yuan et al. 2008). The flux ratio $[O III]/H\beta = 0.1 < 3$ (according to the most recent measurements by Zhou et al. 2006) indicates that the Balmer lines are indeed originated from the usual broad-line region, meaning that this is not a Type II AGN (Zhou et al. 2003). There is no obscured broad-line region, as supported by the absence of any additional absorption in the optical (see the analyses by Zhou et al. 2003, 2006) and X-ray spectra (no additional N_H is required in the fit of Swift/XRT data in the present work; see Sect. 3.2). A reanalysis of SDSS data by Zhou et al. (2006) succeeded in separating the $H\beta$ into a broad and narrow components (see also Rodriguez-Ardila et al. 2000), where the "broad" component has $FWHM = 1432 \pm 87 \text{ km s}^{-1}$. Therefore, PM N J0948+ 0022 has a broad and a narrow line region, but the FWHM of the "broad" lines is small, less than 2000 km s^{-1} .

Its strong and variable radio emission (RL > 1000), together with a flat and inverted radio spectrum ($\alpha_r = -0.24$, with defined as $S_\nu/\nu^{-\alpha_r}$), make PM N J0948+ 0022 one of the few undoubtedly radio-loud narrow-line Seyfert 1 quasars. In addition, VLB I observations at different epochs revealed high brightness temperatures and significant flux density variations, requiring a Doppler factor > 2.5 and a viewing angle $< 22^\circ$ (Doi et al. 2006). Now, a γ ray detection is reported in the first list of bright γ -ray sources (significance $> 10\sigma$) detected by Fermi/LAT (Abdo et al. 2009a) and, specially, in the List of Bright AGN Sources (LBAS, Abdo et al. 2009b).

3. DATA ANALYSIS

3.1. Fermi/LAT

PM N J0948+ 0022 appears in the LBAS derived from the first three months of the Fermi/LAT all-sky survey.

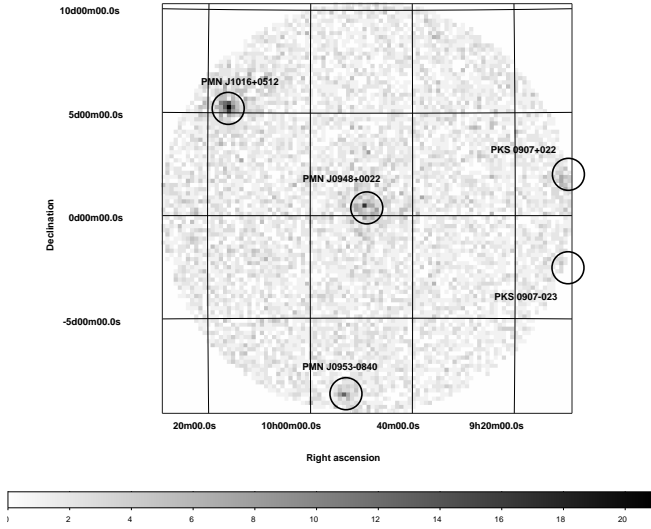


Fig. 1. | Fermi/LAT counts map ($E > 200$ MeV) of the region centered on PKS J0948+0022 with radius 10° . The pixel size is 0.2° . The gray scale bar is in units of LAT counts integrated in the 5-month period. Epoch of coordinates is J2000. Nearby sources included in the likelihood analysis are also indicated.

It is associated (93% confidence level) with the source OGLE J0948.3+0019 (Abdo et al. 2009a,b). In order to improve the positional accuracy for this source and hence increase the confidence level of the association, we added two more months of data to the three months of the LBAS, thus providing 5 months of data (from August through December 2008).

The data from the Large Area Telescope (LAT, Atwood et al. 2008) were analyzed using the Fermi/LAT Science Tools v 9.8.2, a specific LAT software package⁵². In summary, we performed the analysis using the guidelines described in detail in the LBAS paper (Abdo et al. 2009a,b), but with some specific features to best fit the characteristics of this source. Events of "Diverse" class in the Science Tools, coming from zenith angles $< 105^\circ$ (to avoid Earth's albedo) were extracted from a region with a 10° radius centered on the coordinates of the radio position of PMN J0948+0022 (RA = $09^{\text{h}}48^{\text{m}}57^{\text{s}}.6$ and Dec = $+00^{\circ}22'12''.0$, J2000). Because of calibration uncertainties at low energies, data were selected with energies above 200 MeV, with no γ ray detected at energies > 3 GeV. The γ ray background is mainly due to three components: the diffuse emission from the Milky Way, the diffuse extragalactic background and the instrumental background. All these components were modeled and accounted for in the analysis.

An unbinned likelihood algorithm, implemented in the LAT Science Tools as the `gtlike` task, was used to analyze the data. PMN J0948+0022 was modeled together with four other nearby sources: PKS 0907+022, PKS 0907-023, PMN J1016+0512, PMN J0953-0840, to take possible contaminations into account, due to the strongly energy-dependent point-spread function (see Figure 1).

The best fit position of the LAT source, after 5 months of integration, is RA = $09^{\text{h}}48^{\text{m}}58^{\text{s}}$ and Dec =

$+00^{\circ}22'48''.0$ (J2000), with a 95% error radius of $12''36''$ (0.21°) and detection test statistics $TS = 305$ (a 17 detection; see Mattox et al. 1996 for the definition of TS). Figure 1 shows the LAT counts map with the peak of counts consistent with the radio position of PMN J0948+0022. The Figure-of-Merit (FoM) method to associate γ ray sources with known radio counterparts was used (Sowards-Emmerd et al. 2003; Abdo et al. 2009a,b). The value of the FoM increased from 18.64 and 93% confidence level (Bright AGN List, 3 months data) to 53.92 and 99% probability that the association is correct (5 months data).

Fig. 2 (A) displays the light curve for $E > 200$ MeV integrated over 10-day time bins between 1 August 2008, 00 UT, to 1 January 2009, 00 UT (MJD 54679–54832). The corresponding photon indices, defined as $F(E)/E$, are shown in Fig. 2 (B). The light curve indicates clear variability of a factor of ~ 10 over a timescale of weeks, compared with a $\chi^2 = 34.5$ for 14 degrees of freedom ($\chi^2 = 2.5$) for a fit with a constant, and an excess variance of 0.19 ± 0.06 (see Nandra et al. 1997 for a definition of excess variance). On the other hand, the photon index does not show evident variability and can be fitted with a constant ($\chi^2 = 0.80$). The radio data at 15 GHz in Fig. 2 (C), described in Section 3.3, displays no variability during the same time interval. We note, however, that radio data are missing during the episode of variability at γ -rays at the beginning of the LAT lightcurve (Fig. 2 (A)) and a strong radio outburst was observed well before the launch of Fermi.

The spectrum averaged over the whole data set was initially fitted with a single power-law model with $\Gamma = 2.6 \pm 0.1$ and flux ($E > 200$ MeV) equal to $(4.0 \pm 0.3) \times 10^8 \text{ ph cm}^{-2} \text{ s}^{-1}$ ($TS = 298$). A fit with a broken-power law model gives a slight increase of the TS . The spectral parameters are the following: the break energy is $E_b = 1.0 \pm 0.4$ GeV, while the photon index for $E < E_b$ is $\Gamma_1 = 2.3 \pm 0.2$ and for $E > E_b$ is $\Gamma_2 = 3.4 \pm 0.5$. The integrated flux ($E > 200$ MeV) is $(3.9 \pm 0.3) \times 10^8 \text{ ph cm}^{-2} \text{ s}^{-1}$ ($TS = 305$). The likelihood test ratio gives 97% probability in favor of the broken power-law model with respect to the single power-law.

It is worth noting that the quoted errors are statistical only. Systematic errors should be added. According to the studies on the Vela Pulsar (Abdo et al. 2009c), our current conservative estimates of systematic errors are $< 30\%$ for flux measurements and 0.1 for the photon index. Significant reduction of such systematic uncertainties is expected once the calibration of the LAT instrument is completed.

3.2. Swift

On 5 December 2008 at 02:25 UTC (MJD 54805.10), Swift observed PMN J0948+0022 (ObsID 00031306001, exposure ~ 4 ks). For the screening, reduction and analysis of the data from the three instruments (BAT, Barthelmy et al. 2005; XRT, Burrows et al. 2005; UVOT, Roming et al. 2005) onboard the Swift satellite (Gehrels et al. 2004), we used the HEASoft v. 6.6.1 software package, together with the CALDB updated on 9 December 2008.

The X-Ray Telescope XRT (0.2–10 keV energy band) was used in photon counting mode and no evidence of

⁵² <http://fermi.gsfc.nasa.gov/ssc/data/analysis/software/>

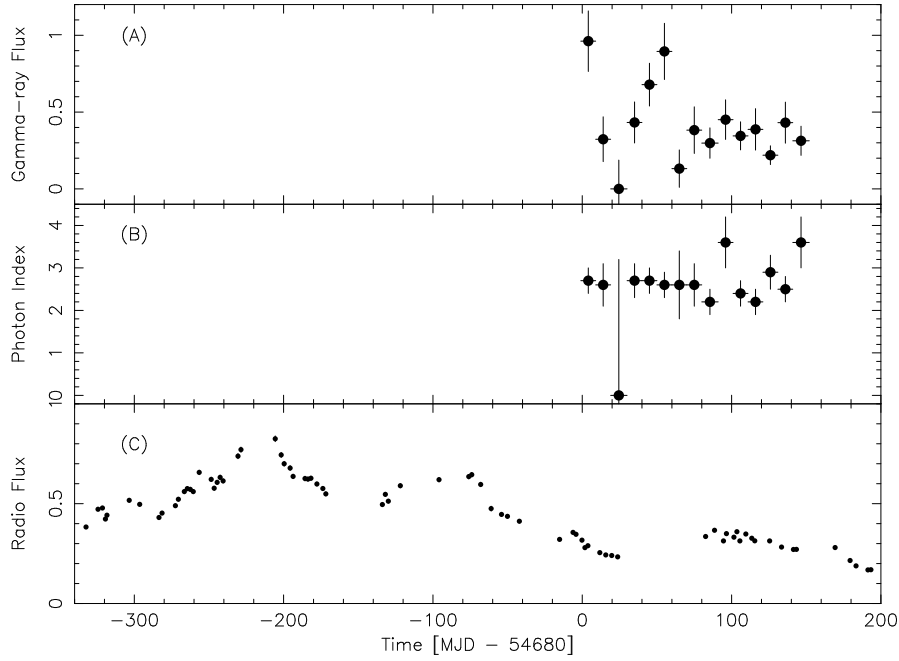


Fig. 2. (panel A) Fermi/LAT flux for $E > 200$ MeV in units of $[10^7 \text{ ph cm}^{-2} \text{ s}^{-1}]$ with 10-day time bins and (panel B) the corresponding photon index. (panel C) OVRO radio flux at 15 GHz [Jy]. Time scale is from 4 September 2007 at 16:25:41 UTC to 11 February 2009 06:53:48 UTC and the day 0 in the X-axis refers to the beginning of LAT observations (1 August 2008).

TABLE 1

Summary of results from analysis of the Swift data obtained on 5 December 2008 (ObsID 00031306001). See the text for details.

BAT (20–100 keV)						
Exposure	Flux _{20–100keV}					
[ks]	[$10^{10} \text{ erg cm}^{-2} \text{ s}^{-1}$]					
4:3	< 7:0					
XRT (0.2–10 keV)						
Exposure	N_{H}^*	Normalization at 1 keV			Flux _{0.2–10keV}	
[ks]	[10^{20} cm^{-2}]	[$10^3 \text{ ph cm}^{-2} \text{ s}^{-1} \text{ keV}^{-1}$]			[$10^{12} \text{ erg cm}^{-2} \text{ s}^{-1}$]	
4:2	5:22	1:83	0:17	1:5	0:3	2:2 0:2
UVOT (observed magnitudes)						
v	b	u	uvw1		uvm2	uvw2
[5468 Å]	[4392 Å]	[3465 Å]	[2600 Å]		[2246 Å]	[1928 Å]
18:2 0:1	18:56 0:07	17:79 0:06	17:48 0:06		17:50 0:06	17:55 0:05

*Fixed value from measurements of the Galactic absorption by the Leiden-Argentine-Bonn survey (Kalberla et al. 2005).

pile-up was found. Data were processed and screened by using the xrt pipeline task with default parameters and grades 0–12 (the single to quadruple pixels events). The spectrum was rebinned to have at least 30 counts per bin.

No detection was found at $E > 10$ keV with BAT, after having binned, cleaned from hot pixels, deconvolved and integrated all the data available in this pointing.

UVOT observed the source with all the six available filters. Data were integrated with the uvotimsum task and then analyzed by using the uvotsource task, with a source region radius of $5''$ for the optical filters and $10''$ for the ultraviolet, while the background was extracted from a circular region $1''$ -sized and centered in a nearby source-free region. It was not possible to select an annular region centered on PM N J0948+ 0022, because of nearby sources. The observed magnitudes were dereddened according to the extinction laws of Cardelli et al. (1989) with $A_V = 0.277$ and then converted into flux

densities according to the standard formulae and zero-points (Poole et al. 2008).

The results are summarized in Table 1.

3.3. Radio

3.3.1. Ebersberg

The centimeter spectrum of PM N J0948+ 0022 was observed with the Ebersberg 100 m telescope on 24 January 2009 (MJD 54855.5) within the framework of a Fermi-related monitoring program of potential γ -ray blazars (F-GAMMA project, Fühmann et al. 2007). The measurements were conducted with the secondary focus heterodyne receivers at 2.64, 4.85, 8.35, 10.45, 14.60 and 32.00 GHz. The observations were performed quasi-simultaneously with cross-scans, that is slewing over the source position, in azimuth and elevation direction, with adaptive numbers of sub-scans for reaching the desired sensitivity (for details, see Fühmann et al. 2008; Angelakis et al. 2008). Pointing offset correction, gain

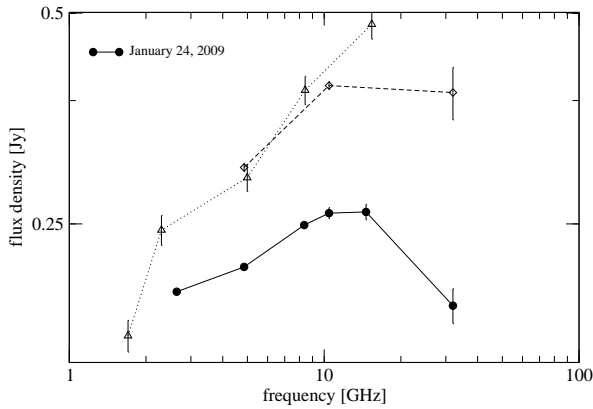


Fig. 3. The evolution of the radio spectrum of PMN J0948+022. Filled circles denote the E-elsberg observations of January 2009. Archival data is shown in grey: triangles represent VLBA measurements conducted in October 2003 (Doi et al. 2006), diamonds represent archival E-elsberg measurements obtained in 2006 (Vollmer et al. 2008).

correction, atmospheric opacity correction and sensitivity correction have been applied to the data.

The acquired radio spectrum has a convex shape with a turnover frequency between 10.45 and 14.60 GHz (Fig. 3). The low-frequency part spectral index $\alpha_{2.64}^{10.45}$, measured between 2.64 and 10.45 GHz, is 0.18 ± 0.02 , whereas the high-frequency optically thin spectral index $\alpha_{14.6}^{32} = 0.39$.

The comparison of the acquired spectrum with previously observed ones (Vollmer et al. 2008, Doi et al. 2006) reveals that the source is presently in a much lower flux density state (see Fig. 3). This indicates intense variability. From the change of the 4.85 GHz flux density over about three years (Vollmer et al. 2008) we estimate a variability brightness temperature (e.g. Fuhmann et al. 2008) of 1.4×10^{11} K. Assuming the equipartition brightness temperature limit of 10^{11} K (Readhead et al. 1994), we obtain a lower limit for the Doppler factor of > 1.4 .

3.3.2. Owens Valley Radio Observatory (OVRO)

PMN J0948+0022 has been observed regularly from 4 September 2007 at 16:25 UTC to 11 February 2009 06:53 UTC (MJD 54347.68–54873.29) at 15 GHz by the Owens Valley Radio Observatory (OVRO) 40 m telescope as part of an ongoing Fermi blazar monitoring program of all 1159 CGRABs blazars north of declination ~ 20 degrees (Healey et al. 2008). Flux densities were measured using azimuth double switching as described in Readhead et al. (1989). The relative uncertainties in flux density result from a 5 mJy typical thermal uncertainty in quadrature with a 1.6% systematic uncertainty. The absolute flux density scale is calibrated to about 5% using the model for 3C 286 by Baars et al. (1977). This absolute uncertainty is not included in the plotted errors.

PMN J0948+0022 has been reported to show variability by a factor of 2 in radio over year time-scales (Zhou et al., 2003) and 31% fluctuations in month time-scales (Doi et al., 2006). The OVRO 40 m 15 GHz time series shows clear structure at timescales down to weeks, and year-scale fluctuations by a factor of 4 (Fig. 2, panel C). The rapid variability we observe in this object { at least

400 mJy in 77 days or 5 mJy/day { enables us to determine a variability brightness temperature of $\sim 2 \times 10^{13}$ K, assuming the Λ CDM cosmology described in Sect. 1.

It is often not easy to determine the optically thin spectral index of blazars at radio frequencies because they are complex structures, with different regions becoming optically thin at different radio frequencies. In the present case the most recent results show a turnover between 10 and 15 GHz, and a 15–30 GHz spectral index of

0.4, but we do not believe that this is the optically thin spectral index. It is much more likely that one is still seeing synchrotron self-absorption so that the spectrum between 15 GHz and 30 GHz is much flatter than the true optically thin spectral index. In such cases, it is safer to assume an optically thin spectral index of 0.75 and to use the frequency of observation. These only have a small effect on the derived T_{eq} unless δ is very close to 0.5, which is too flat, in our view, for an optically thin spectral index in most cases.

The equipartition brightness temperature (Readhead, 1994), in the current cosmological model, is then $T_{\text{eq}} = 5.5 \times 10^{10}$ K, assuming an average optically thin spectral index of 0.75, and hence the equipartition Doppler factor is ~ 7 , which is typical of highly variable blazars. This agrees with Doi et al. (2006), who reported an equipartition Doppler factor > 2.7 , and the E-elsberg lower limit reported in Sect. 3.3.1. This suggests that, in the compact radio emission regions in this object, the Lorentz factor is of order 10.

4. SPECTRAL ENERGY DISTRIBUTION (SED)

Fig. 4 displays the spectral energy distribution (SED) built with the Fermi/LAT, Swift, and E-elsberg and OVRO data analyzed in the present work (red symbols) together with archival data (green symbols). Archival radio data are from Bennett et al. (1986), Becker et al. (1991), Gregory & Condon (1991), White & Becker (1992), Griith et al. (1995), Doi et al. (2006); optical/IR data are from USNO B1 for B, R, I filters (Monet et al. 2003) and from 2MASS for J, H, K filters (Cutri et al. 2003).

The resulting SED strongly resembles that of a typical high power blazar, with two non-thermal emission peaks in the far IR and between 10^{22} – 10^{23} Hz (40–400 MeV). Also the peak produced by the accretion disk is well defined, due to the UVOT data, extending the photometric coverage to the near UV. If we assume a standard Shakura & Sunyaev (1973) disk emission, the UVOT data permit fixing a lower limit to the mass of the black hole, which turns out to be around $10^8 M_{\odot}$, in agreement with the estimates by Zhou et al. (2003). For lower masses, in fact, the luminosity needed to fit these data becomes super-Eddington.

We model the contemporaneous optical to γ -ray data with a one-zone synchrotron and inverse Compton model, in accordance with the models generally used for blazars. Also for this source, the radio emission is assumed to come from larger-scale emission regions further away along the jet, while the rest of the SED is attributed to the region at the beginning of the jet plus the contribution of the accretion disk. The IR radiation produced by the assumed torus does not influence the derived non-thermal SED, since the corresponding radiation energy density is much smaller than the one produced by the

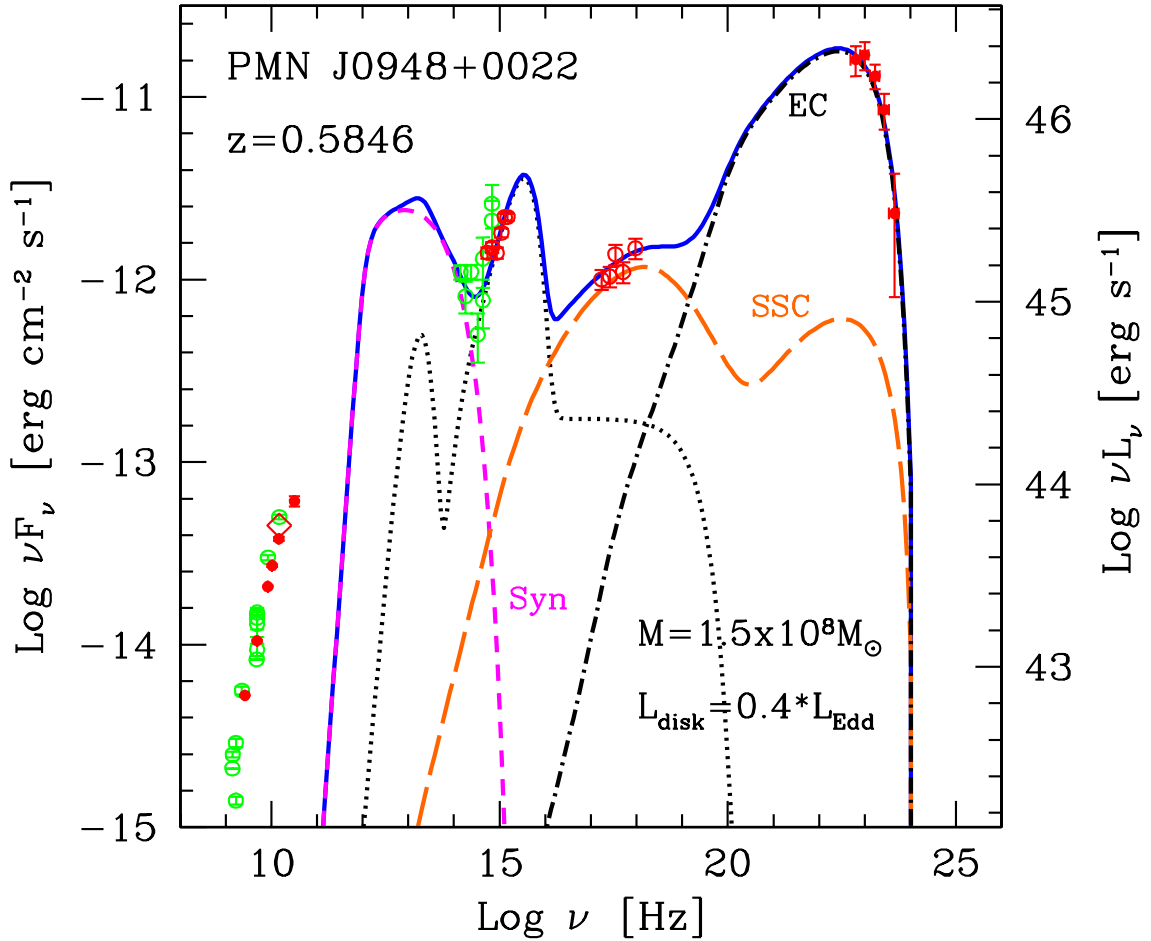


Fig. 4. | Spectral Energy Distribution of PMN J0948+0022. Fermi/LAT (5-months data); Swift XRT and UVOT (5 December 2008); Elvisberg (24 January 2009) and OVRO (average in the 5-months of LAT data, indicated with a red diamond) are indicated with red symbols. Archival data are marked with green symbols. Radio data: from 1.4 to 15 GHz from Bennett et al. (1986), Becker et al. (1991), Gregory & Condon (1991), White & Becker (1992), Griith et al. (1995), Doi et al. (2006). Optical/IR: USNO B1, B, R, I filters (Monet et al. 2003); 2MASS J, H, K filters (Cutri et al. 2003). The dotted line indicates the contributions from the infrared torus, the accretion disk and the X-ray corona. The synchrotron (self-absorbed) is shown with a small dash line. The SSC and EC components are displayed with dashed and dot-dashed lines, respectively. The continuous line indicates the sum of all the contributions.

lines.

The complete description of the general model used can be found in Ghisellini & Tavecchio (2009); here we briefly summarize the main parameters:

the source is assumed to be located at a distance $R_{\text{diss}} = 6.75 \cdot 10^{16}$ cm from a black hole of mass $M = 1.5 \cdot 10^8 M_{\odot}$;

the source is assumed to be a sphere, of radius $R = 6.75 \cdot 10^{15}$ cm (i.e. a conical jet of semiaperture angle $\theta = 0.1$ rad is assumed);

it moves with a bulk Lorentz factor $\Gamma = 10$ at a viewing angle $\nu = 6$;

the disk luminosity is 40% of the Eddington value ($L_{\text{disk}} = 9 \cdot 10^{45}$ erg s $^{-1}$);

above (and below) the disk we assume an X-ray emitting corona, producing a luminosity $L_{\text{cor}} = 0.3 L_{\text{disk}}$ and with a power law spectrum (energy index $\alpha_x = 1$), ending in an exponential cut at 150 keV;

10% of the disk emission is assumed to be absorbed and re-emitted by the broad-emission line region (BLR), which emits narrow permitted lines, in this specific case;

the BLR is placed at a distance $R_{\text{BLR}} = 10^{17} L_{\text{disk},45}^{1/2} = 3 \cdot 10^{17}$ cm, where $L_{\text{disk},45}$ is the disk luminosity in units of 10^{45} erg s $^{-1}$;

a dusty torus absorbs 10% of L_{disk} re-emitting it in the far-IR. Its distance is assumed to be

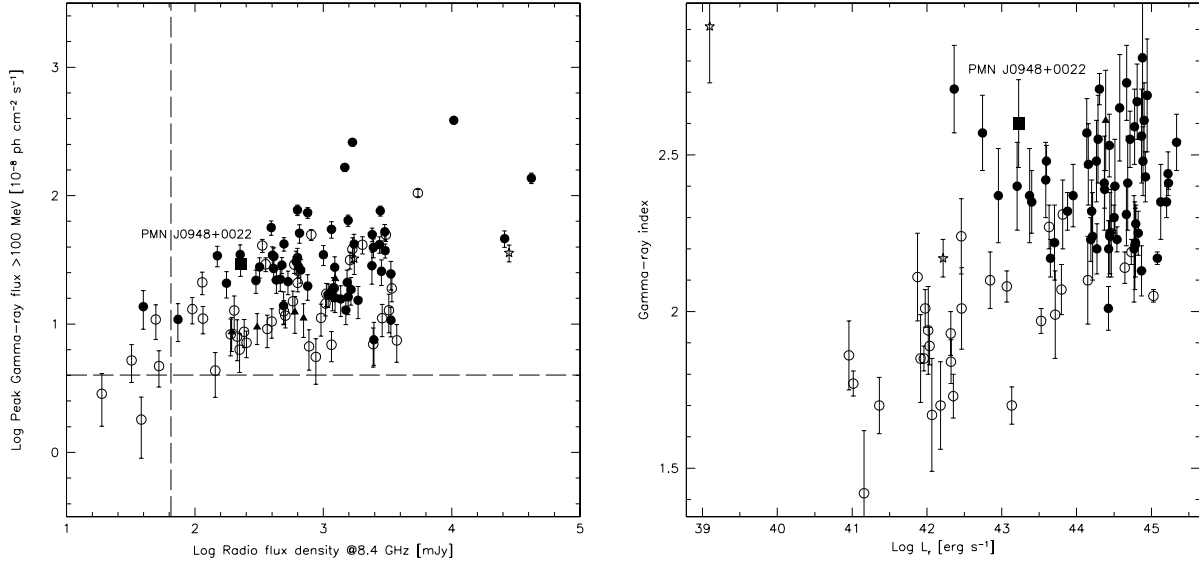


Fig. 5. | Radio versus γ -ray properties of PMN J0948+0022 (indicated with a filled square) compared with the other blazars detected by LAT (figure adapted from Fig. 14 in Abdo et al. 2009b). (left panel) Peak γ -ray flux ($E > 100$ MeV) vs. radio flux density at 8.4 GHz; the dashed lines show the CRATES flux density limit and the typical LAT detection threshold. (right panel) γ -ray photon index vs. radio luminosity.

$R_{\text{IR}} = 2.5 \cdot 10^{18} L_{\text{disk},45}^{1=2} \text{ cm}$, calculated by considering that the dust is at the temperature of 370 K (see Cleary et al. 2007), where is the maximum of efficiency in reprocessing the impinging photons into IR radiation.

For the above choice of parameters, the BLR is the main producer of the seed photons for the inverse Compton scattering in the emitting region. In Fig. 4, this component is labeled EC. On the other hand, the Synchrotron Self-Compton (SSC) radiation is important in the X-ray band, where it dominates the radiative output (the two-peak shape of the SSC curve correspond to the first and second order scattering). In this scenario, i.e. with the X-ray data due to the SSC emission, the magnetic field B is strongly constrained, since it controls the value of the SSC emission. In our case $B = 3.2$ G.

The particle energy distribution of the emitting electrons is calculated by the continuity equation, assuming the injected electrons are distributed in energy according to a smoothly joining broken power law of slopes α_1 and α_2 below and above $\gamma = 800$, respectively. The maximum electron energy corresponds to a random Lorentz factor of $\gamma_{\text{max}} = 1600$ and the inverse-Compton peak corresponds to $\gamma_{\text{peak}} = 411$. The total power injected in the form of relativistic electrons is $L_e^0 = 2.4 \cdot 10^{43} \text{ erg s}^{-1}$, as calculated in the comoving frame.

Once accelerated, the bulk kinetic power carried by the electrons in the jet is $L_e = 5.0 \cdot 10^{44} \text{ erg s}^{-1}$, to be compared with the Poynting flux $L_B = 1.8 \cdot 10^{44} \text{ erg s}^{-1}$ and the power in radiation, $L_{\text{rad}} = 2.0 \cdot 10^{45} \text{ erg s}^{-1}$. As occurs in typical powerful blazars (see e.g. Celotti & Ghisellini 2008, also for the exact definitions of these powers), the radiation observed carries more power than what is available in magnetic field and electron energy. Thus we require that the jet also carries protons: if we assume one proton per electron, we obtain $L_p = 4.8 \cdot 10^{46} \text{ erg s}^{-1}$. This value can be reduced, by assuming

the presence of pairs.

The impact of the presence of narrow permitted lines in the BLR can be evaluated in two ways. First, there can be a geometrical explanation: if the BLR is torus-like and we are observing it face-on, then the Doppler broadening is reduced and the line width is smaller than usual. A similar geometry has been invoked by Decarli et al. (2008) to explain why NLS1 have not small masses.

This BLR geometry, although different from what used in the adopted model, does not affect any of the model results, since the important parameter is the angle at which the jet sees the BLR. Second, it is still possible to consider an isotropic geometry of the BLR and take into account the effect of the radiation pressure, as proposed by Marconi et al. (2008). The BLR is then moved farther from the central singularity ($R_{\text{BLR}} = 5 \cdot 10^{17} \text{ cm}$), but the impact in the model parameters mainly results in an increase of α from 10 to 13. Other new values of parameters are: $\gamma_{\text{max}} = 1500$, $\gamma_{\text{peak}} = 430$, $L_e^0 = 2.6 \cdot 10^{43} \text{ erg s}^{-1}$, $B = 2.01$ Gauss. The power output of the jet is: $L_e = 1.2 \cdot 10^{45} \text{ erg s}^{-1}$, $L_B = 1.3 \cdot 10^{44} \text{ erg s}^{-1}$, $L_{\text{rad}} = 3.2 \cdot 10^{45} \text{ erg s}^{-1}$, $L_p = 7.9 \cdot 10^{46} \text{ erg s}^{-1}$.

It is worth noting that the systematics in the LAT data do not affect significantly the results of the modeling. Indeed, in the case of a LAT flux equal to the 130% of the observed value (the worst case), it is sufficient to increase a little the injected power L_e^0 (from $2.4 \cdot 10^{43}$ to $2.8 \cdot 10^{43} \text{ erg s}^{-1}$) and to decrease a little the magnetic field B (from 3.2 to 2.5 Gauss). The derived quantities become $L_e = 6.3 \cdot 10^{44} \text{ erg s}^{-1}$, $L_B = 1.0 \cdot 10^{44} \text{ erg s}^{-1}$, $L_{\text{rad}} = 2.5 \cdot 10^{45} \text{ erg s}^{-1}$, $L_p = 5.0 \cdot 10^{46} \text{ erg s}^{-1}$. A change in the γ -ray photon index equal to 0.1 results in very negligible changes in the SED.

The model parameters used to explain the SED of PMN J0948+0022 are rather well constrained, given the basic assumptions of the model. However, they may not be unique. Another solution might be possible if we as-

sume that the dusty torus contributing to the IR seed photons is hotter and more compact than assumed here. It must be hotter because otherwise we need too energetic electrons to emit the hard X-ray emission (by EC), and these very same electrons would overproduce (by synchrotron) the observed emission in the optical. A stratified and clumpy torus (e.g. Nenkova et al. 2008) could work. Also in this "hot and clumpy torus" case we can obtain a reasonable representation of the data (i.e. the same ratios between the radiation energy densities (both by synchrotron and external photons (and the magnetic energy density), at distances one order of magnitude larger than assumed here. As a consequence, the emitting region should be one order of magnitude larger, and thus should vary on longer timescales. The detection of a typical variability timescale can therefore discriminate between the two possible solutions.

5. DISCUSSION AND CONCLUSIONS

Our findings show clearly that PM N J0948+ 0022, the first narrow-line quasar detected in γ -rays, hosts a relativistic jet with SED very similar to those of "classical" FSRQ.

The parameters relevant for the spectral shape of the SED derived from the modelling, using the approach by Ghisellini and Tavecchio (2009), are consistent with those of high-power blazars, though at the lower limit in power of the FSRQ region as derived, for example, in Celotti & Ghisellini (2008) for a large sample of blazars (cf. their Fig. 2 and Fig. 6). The comparison of radio vs γ -ray properties shows that in both bands PM N J0948+ 0022 has a relatively low power with respect to the other FSRQ detected by LAT to date, although no striking differences appear (Fig. 5). Eeelsberg and OVRO radio observations also show characteristics similar to those of FSRQ.

We believe that PM N J0948+ 0022 could be one of the first examples of a FSRQ with relatively small mass but high accretion rate in terms of Eddington ratio. This would fit well with the scenario in which the transition between high peaked and low peaked blazars is not related to absolute power but to the Eddington ratio as indicated by the FR I-FR II separation which depends on

mass. It remains to be seen whether the jets in other radio-loud NLS1 conform to this scenario. Fermi is expected to answer this question by measuring the γ -ray luminosity and spectra of the most radio-loud ones.

The Fermi/LAT Collaboration acknowledges generous ongoing support from a number of agencies and institutes that have supported both the development and the operation of the LAT as well as scientific data analysis. These include the National Aeronautics and Space Administration and the Department of Energy in the United States, the Commissariat à l'Énergie Atomique and the Centre National de la Recherche Scientifique / Institut National de Physique Nucléaire et de Physique des Particules in France, the Agenzia Spaziale Italiana and the Istituto Nazionale di Fisica Nucleare in Italy, the Ministry of Education, Culture, Sports, Science and Technology (MEXT), High Energy Accelerator Research Organization (KEK) and Japan Aerospace Exploration Agency (JAXA) in Japan, and the K.A.W. Allenberg Foundation, the Swedish Research Council and the Swedish National Space Board in Sweden.

Additional support for science analysis during the operations phase from the following agencies is also gratefully acknowledged: the Istituto Nazionale di Astrofisica in Italy and the K.A.W. Allenberg Foundation in Sweden for providing a grant in support of a Royal Swedish Academy of Sciences Research fellowship for JC.

This research is partly based on observations with the 100-m telescope of the MPIfR (Max-Planck-Institut für Radioastronomie) at Eeelsberg. The monitoring program at the OVRO is supported by NASA award NNX08AW31G and NSF award AST-0808050.

This research has made use of the NASA/IPAC Extragalactic Database (NED) which is operated by the Jet Propulsion Laboratory, California Institute of Technology, under contract with the National Aeronautics and Space Administration. This research has made use of data obtained from the High Energy Astrophysics Science Archive Research Center (HEASARC), provided by NASA's Goddard Space Flight Center.

REFERENCES

- Abdo A.A., Ackermann M., Ajello M., et al., 2009a, *ApJ*, accepted [arXiv:0902.1340]
 Abdo A.A., Ackermann M., Ajello M., et al., 2009b, *ApJ*, accepted [arXiv:0902.1559]
 Abdo A.A., Ackermann M., Atwood W.B., et al., 2009c, *ApJ*, 696, 1084
 Aharonian F., Akhperjanian A.G., Barres de Almeida U., et al., 2008, *A & A*, 478, 387
 Atwood W.B., Abdo A.A., Ackermann M., et al., 2009, *ApJ*, 697, 1071
 Angelakis E., Fuhmann L., Marchilli N., Krichbaum T.P., & Zensus J.A., 2008, *Mém. SAIt*, 79, 1042
 Baars J.W.M., Genzel R., Pauliny-Toth I.I.K. & Witzel A., 1977, *A & A*, 61, 99
 Barthelmy S.D., Barbier L.M., Cummings J.R., et al., 2005, *Space Science Review*, 120, 143
 Becker R.H., White R.L. & Edwards A.L., 1991, *ApJS*, 75, 1
 Bennett C.L., Lawrence C.R., Burke B.F., Hewitt J.N., Mahoney J., 1986, *ApJS*, 61, 1
 Blandford R. & Rees M., 1978, In: *Pittsburgh Conference on Black Hole Objects*, A.N. Wolfe (ed), Pittsburgh University Press, p. 328
 Blandford R.D. & Levinson A., 1995, *ApJ*, 441, 79
 Blazejowski M., Sikora M., Moderski R. & Madejski G., 2000, *ApJ*, 545, 107
 Boroson T.A., 2002, *ApJ*, 565, 78
 Bottcher M. & Deemer C.D., 2002, *ApJ*, 564, 86
 Burrows D.N., Hill J.E., Nousek J.A., et al., 2005, *Space Science Review*, 120, 165
 Cardelli J.A., Clayton G.C., Mathis J.S., 1989, *ApJ*, 345, 245
 Cavaliere A. & D'Elia V., 2002, *ApJ*, 571, 226
 Celotti A. & Ghisellini G., 2008, *MNRAS*, 385, 283
 Cleary K., Lawrence C.R., Marshall J.A., et al., 2007, *ApJ*, 660, 117
 Cutri R.M., Skrutskie M.F., van Dyk S., et al., 2003, *The IRSA 2MASS All-Sky Point Source Catalog*, NASA/IPAC Infrared Science Archive.
 Decarli R., Otti M., Fontana M., Haardt F., 2008, *MNRAS*, 386, L15
 Deemer C.D., Schlickeiser R. & Mastichiadis A., 1992, *A & A*, 256, L27
 Doi A., Nagai H., Asada K., et al., 2006, *PA SJ*, 58, 829
 Falcone A.D., Bond I.H., Boyle P.J., et al., 2004, *ApJ*, 613, 710
 Fender R. & Belloni T., 2004, *ARA & A*, 42, 317

- Foschini L., Maraschi L., Tavecchio F., et al., 2009, *Adv. Space Res.*, 43, 889
- Fossati G., Maraschi L., Celotti A., Comastri A. & Ghisellini G., 1998, *MNRAS* 299, 433
- Fuhrmann L., Zensus J.A., Krichbaum T.P., Angelakis E., & Readhead A.C.S., 2007, *The First GLAST Symposium*, 921, 249
- Fuhrmann L., et al., 2008, *A & A*, 490, 1019
- Gehrels N., Chincarini G., Giommi P., et al., 2004, *ApJ*, 611, 1005
- Ghisellini G., Maraschi L. & Treves A., 1985, *A & A*, 146, 204
- Ghisellini G., Celotti A., Fossati G., Maraschi L. & Comastri A., 1998, *MNRAS* 301, 451
- Ghisellini G. & Celotti A., 2001, *A & A*, 379, L1
- Ghisellini G. & Tavecchio F., 2008, *MNRAS*, 387, 1669
- Ghisellini G. & Tavecchio F., 2009, *MNRAS*, in press [arXiv:0902.0793]
- Gregory P.C. & Condon J.J., 1991, *ApJS*, 75, 1011
- Gri th M.R., Wright A.E., Burke B.F. & Ekers R.D., 1995, *ApJS*, 97, 347
- Healey S.E., Romani R.W., Cotter G., et al., 2008, *ApJS*, 175, 97
- Kalberla P.M.W., Burton W.B., Hartmann D., et al., 2005, *A & A*, 440, 775
- Komatsu E., Dunkley J., Nolte M.R., et al., 2009, *ApJS*, 180, 330
- Komossa S., Voges W., Xu D., et al., 2006, *ApJ*, 132, 531
- Maraschi L., 2001, In: *20th Texas Symposium on Relativistic Astrophysics*, *AP Conference Proceedings* 586, J.C. Wheeler and H. Martel (eds), p.409
- Maraschi L. & Tavecchio F., 2001, In: *Blaazar Demographics and Physics*, *ASP Conference Series* 227, P. Padovani & C. M. Urry (eds), p.40
- Maraschi L. & Tavecchio F., 2003, *ApJ*, 593, 667
- Maraschi L., Foschini L., Ghisellini G., Tavecchio F., Sambruna R.M., 2008, *MNRAS*, 391, 1981
- Marconia A., Axon D.J., Aiello R., et al., 2008, *ApJ*, 678, 693
- Mattox J.R., Bertsch D.L., Chiang J.L., et al., 1996, *ApJ*, 461, 396
- Monet D.G., Levine S.E., Casian B., et al., 2003, *AJ*, 125, 984
- Nandra K., George I.M., Ushotzky R.F., Tumer T.J. & Yaqoob T., 1997, *ApJ*, 476, 70
- Nenkova M., Sirocky M., Ivezić Z., Eitzur M., 2008, *ApJ*, 685, 147
- Padovani P., 2007, *Astrophys. Space Sci.*, 309, 63
- Pogge R.W., 2000, *New Astronomy Review*, 44, 381
- Poole T.S., Bevelde A.A., Page M.J., et al., 2008, *MNRAS*, 383, 627
- Readhead A.C.S., Lawrence C.R., Myers S.T., et al., 1989, *ApJ*, 346, 566
- Readhead A.C.S., 1994, *ApJ*, 426, 51
- Rees M.J., 1966, *Nature*, 211, 468
- Rodríguez-Ardila A., Binette L., Pastoriza M.G., Donzelli C.J., 2000, *ApJ*, 538, 581
- Rom ing P.W.A., Kennedy T.E., Mason K.O., et al., 2005, *Space Science Review*, 120, 95
- Shakura N.I. & Sunyaev R.A., 1973, *A & A*, 24, 337
- Sikora M., Begelman M.C. & Rees M.J., 1994, *ApJ*, 421, 153
- Sowards-Emmert D., Romani R.W. & Michelson P.F., 2003, *ApJ*, 590, 109
- Urry C.M. & Padovani P., 1995, *PASP*, 107, 803
- Vollmer B., Krichbaum T.P., Angelakis E. & Kovalev Y.Y., 2008, *A & A*, 489, 49
- White R.L. & Becker R.H., 1992, *ApJS*, 79, 331
- Yuan W., Zhou H.-Y., Komossa S., et al., 2008, *ApJ*, 685, 801
- Zhou H.-Y., Wang T.-G., Dong X.-B., et al., 2003, *ApJ*, 584, 147
- Zhou H.-Y., Wang T.-G., Yuan W.-M., et al., 2006, *ApJS*, 166, 128